



*Annual Review of Condensed Matter Physics*  
**Multiphase-Field Models  
of Tissues**

Siavash Monfared, Aleksandra Ardaševa,  
and Amin Doostmohammadi

Niels Bohr Institute, University of Copenhagen, Copenhagen, Denmark;  
email: doostmohammadi@nbi.ku.dk

Annu. Rev. Condens. Matter Phys. 2026. 17:91–113

The *Annual Review of Condensed Matter Physics* is  
online at [commatphys.annualreviews.org](http://commatphys.annualreviews.org)  
<https://doi.org/10.1146/annurev-commatphys-060625-061354>

Copyright © 2026 by the author(s).  
All rights reserved

**Keywords**

biological physics, multicellular systems, cell collectives, self-organization, active matter, tissue mechanics

**Abstract**

Understanding how cells coordinate their behaviors to produce large-scale patterns and functions is central to deciphering biological processes ranging from tissue development and regeneration to cancer progression and morphogenesis. Despite advances in imaging and mechanical characterization, the role of physical forces in collective cell dynamics remains incompletely understood. Physics-based models are essential for complementing experimental data, offering access to high-resolution spatiotemporal fields, and enabling mechanistic insights into complex multicellular systems. This review focuses on dense, soft tissues, in which the mechanical deformation of one cell drives reorganization of its neighbors, giving rise to emergent behaviors such as orientational order and long-range force transmission. The multiphase-field model provides a powerful and versatile framework to investigate such systems, bridging biological phenomena and the nonequilibrium physics of active matter. We discuss the theoretical foundations of the model and its applications to a range of biological contexts, including cell migration, heterogeneous populations, confined geometries, and metastasis. We also emphasize the integration of simulations with experimental data, highlighting how this approach is reshaping our understanding of tissue mechanics, collective order, and force transmission. Finally, we outline current trends and future challenges in applying multiphase-field models to biology and soft matter physics.



## 1. INTRODUCTION

Concluding the case for his theory of evolution, Charles Darwin wrote (1) in *On the Origin of Species*, “from so simple a beginning endless forms most beautiful and most wonderful have been, and are being, evolved.” Darwin was discussing the evolution of diverse lifeforms from one ancestral organism, but just as magical is the development of a complex multicellular organism from a single parent cell. This process is a highly orchestrated affair that cells conduct collectively without any central guidance, creating intricate dynamic patterns essential to development and regeneration. However, despite the remarkable advances in imaging spatiotemporal dynamics of cell collectives and techniques for mechanical characterization both *in vivo* and *in vitro* (2–6), the role of physical forces on biological functions remains poorly understood. In this vein, physics-based models play a critical role in complementing experiments, providing access to high-resolution spatiotemporal fields in three dimensions. A particularly important but challenging system to study is a dense, soft multicellular one, such as tissues, where mechanical deformation of one cell necessitates reorganization of neighboring cells. It is within this context that a multiphase-field model shines, offering a rich physics-based framework to advance our understanding of biological systems while providing a robust playground for nonequilibrium statistical physics.

This review is organized as follows: We begin with an introduction to physical models for cell collectives, highlighting the importance of understanding collective cell behavior in development and regeneration. Next, we delve into the multiphase-field model, discussing its foundational aspects, including timescale separability, free energy functionals for passive interactions, and nonequilibrium behavior driven by active processes. We then explore the physics of active matter, focusing on collective self-organization, topological defects, active stress chains, and the emergence of biological phenomena. In the subsequent section, we bridge biological physics with experimental integration, covering quantitative modeling informed by experiments, cell migration in two and three dimensions, heterogeneous cell populations, and confined systems. Finally, we conclude with a discussion of current trends, the importance of multiphase-field models in biological and physics research, and future challenges.

Due to their ability to incorporate changes in shape, cell–cell, and cell–substrate interactions, as well as subcellular details, phase-field models have provided valuable theoretical predictions of the biophysics of single cells that have been tested experimentally (reviewed in 7). Throughout, we emphasize the role of physics-based models in advancing our understanding of multicellular systems while noting that this review does not address single-cell modeling, molecular-level dynamics, or nonbiological applications of multiphase-field models.

Multicellular assemblies are integral to numerous biological processes, including tissue formation (4, 8), wound healing (9, 10), and cancer metastasis (11, 12). These assemblies, composed of interacting cells, exhibit complex behaviors essential for the proper functioning of biological systems. Understanding and modeling these behaviors are crucial to the advancement of fields such as developmental biology, regenerative medicine (13, 14), and cancer research (15, 16).

One of the primary challenges in studying multicellular assemblies is the inherent complexity of the multibody physics problem. Each cell within an assembly is constantly changing shape and dynamically interacting with its neighbors and the extracellular environments. These interactions are highly nonlinear and multiscale in nature, including adhesion, repulsion, and mechanical stress due to deformation. Additionally, cells can produce work, migrate, divide, and extrude, further complicating the modeling process.

Although this review focuses on the latest advances in multiphase-field models and their application to living cells, it is worth briefly discussing other types of approaches. A more comprehensive overview can be found elsewhere (7, 17–19): (a) Active network models include



vertex-based (20) and Voronoi-based (21) approaches that, in most cases, represent a confluent layer through geometric description of each cell and the associated effective energy functional for the work required to deform that cell. Two-dimensional (2D) active network models have played a key role in explaining some of the fundamental biological observations (22, 23) with recent advances extending the model into the third dimension (24) and more complex force generation mechanisms (25). (b) Particle-based models for living cells are based on granular physics concepts. These models have been instrumental in studying collective motion emerging from local interactions and force generation mechanisms (26–28). However, this approach cannot capture cell shape changes (deformation), which is critical for modeling dense, deformable multicellular assemblies. (c) Cellular Potts models (29) represent another paradigm for modeling cellular systems in which each cell is defined as a spin collection. These models can provide detailed descriptions of cell shapes. However, these shapes can be affected by artifacts due to the lattice choice. Furthermore, shape fluctuations depend on a temperature parameter that cannot be directly calibrated against experimental measurements. (d) Continuum models (30–36) typically leverage hydrodynamics and have been instrumental in modeling the behavior of cell collectives. However, they provide a coarse-grained description of an inherently discrete system, and are thus unable to resolve individual cell shapes as well as local force, and density fluctuations that are now understood to be fundamental to many biological functions. Such insights are less likely to be obtained from mean-field descriptions of relevant fields.

The multiphase-field model overcomes some of these limitations. It can naturally handle deformable interfaces and efficiently scale to a large system in three dimensions, which is a necessity for understanding inherently three-dimensional (3D) biological processes such as embryogenesis and tumorigenesis. Furthermore, its discrete nature, at the scale of an individual cell, can capture large fluctuations while providing a robust way to model proliferation, genetic mutations, and/or expressions. This framework is also able to represent an arbitrary level of confluence (37–39) and is rather flexible in incorporating various passive and active interactions in a concise and consistent manner. As such, the multiphase-field model provides a robust framework to establish an integrated understanding of living matter as an interplay among mechanical cues, genetics, and biochemical signals.

## 2. MULTIPHASE-FIELD MODEL

Early phase-field models for modeling cells focused on single and multicomponent vesicles (40, 41) and single-cell morphodynamics (42–45). This was followed by models for cell collectives (37, 46–49), including a number of 3D multiphase-field models that offer unprecedented insights into the physics of cell collectives (50–53).

In the multiphase-field modeling approach, each cell is represented as an active droplet interacting with a surface. Generally in such a system, the drag due to the surface interactions dominates, leading to overdamped (translational) dynamics. Without loss of generality, consider a cellular monolayer that consists of  $N$  cells on a rigid substrate with its surface normal  $\vec{e}_n$  ( $= \vec{e}_z$ )  $= \vec{e}_x \times \vec{e}_y$  and periodic boundaries in both  $\vec{e}_x$  and  $\vec{e}_y$ , where  $(\vec{e}_x, \vec{e}_y, \vec{e}_z)$  constitute the global orthonormal basis. Each cell  $i$  is represented by a 3D phase-field  $\phi_i = \phi_i(\vec{x}, t)$ . Interface dynamics is modeled via this auxiliary phase-field order parameter that varies smoothly between the inside and outside of each cell domain. Such a construct eliminates the need for explicitly defining and tracking the interface spatiotemporally while providing the resolution necessary to resolve intercellular interactions. In turn, this leads to a highly scalable framework suitable for studying emerging behavior in large systems of interacting cells, such as tissues and organs. Furthermore, the free energy functional at the core of a phase-field model provides a versatile and elegant



mathematical and thermodynamically consistent framework to model a wide range of physico-chemical interactions.

## 2.1. Timescale Separability: Translational and Relaxational Dynamics

Formation of an embryo (54, 55), tissue repair (56, 57), and metastasis (58–60) emerge from collective interactions of living cells. This involves coordinated regulation of cell shape deformation and motion in space and time, without any central guidance, leading to an inherently multi-scale process, ranging from molecular to multicellular length scales and spanning timescales from milliseconds to days (61).

One way to approach modeling the collective self-organization in living cells is to consider two subproblems: *(a)* translational dynamics associated with cell movement and *(b)* relaxational dynamics associated with cell deformation. Implicit in this approach is the assumption that the dynamics associated with each subproblem satisfies timescale separability. This is indeed a justified assumption based on experimental characterizations of cell shape relaxation (62). This paves the way to decouple two partial differential equations, one describing the (relatively) fast dynamics of relaxation and the other concerned with (relatively) slow dynamics of translation. For the translational dynamics, an overdamped Langevin-type dynamics can be considered:

$$\xi \vec{v}_i(\vec{x}, t) = \vec{F}_i^{\text{active}}(\vec{x}, t) + \vec{F}_i^{\text{passive}}(\vec{x}, t), \quad 1.$$

where  $\xi$  parameterizes substrate friction (here considered a constant but can depend on space and time); and  $\vec{F}_i^{\text{passive}}$ ,  $\vec{F}_i^{\text{active}}$ , and  $\vec{v}_i$  represent, respectively, passive forces, active forces, and velocity for cell  $i$ , itself represented by  $\phi_i$ . By contrast, the relaxational dynamics of the interface is described by a time-dependent Ginzburg–Landau model, also known as model A dynamics in the Hohenberg–Halperin classification scheme (63), with an extra advective term:

$$\partial_t \phi_i + \vec{\nabla} \cdot (\vec{v}_i \phi_i) = -\Gamma \frac{\delta \mathcal{F}}{\delta \phi_i}, \quad i = 1, \dots, N, \quad 2.$$

where  $\phi_i(\vec{x}, t)$  is a scalar field representing the interface associated with cell  $i$ .  $\Gamma$  is the mobility coefficient, affecting the relaxation timescale, and  $\mathcal{F}$  represents the free energy functional. Furthermore, we assume a nearly incompressible system, i.e.,  $\vec{\nabla} \cdot \vec{v}_i \approx 0$ , and thus the advective term  $\vec{\nabla} \cdot (\vec{v}_i \phi_i) \approx \vec{v}_i \cdot \vec{\nabla} \phi_i$  updates the field  $\phi_i(\vec{x}, t)$  for each time step and each cell  $i$ .

## 2.2. Free Energy Functional: Passive Interactions

Generally, passive forces derive from the energy minimization principle obeying detailed balance and time-reversal symmetry. To this end, one can define passive forces acting on each cell,  $\vec{F}_i^{\text{passive}}$ , as follows:

$$\vec{F}_i^{\text{passive}} = \int d\vec{x} \left( \sum_i^N \frac{\delta \mathcal{F}}{\delta \phi_i} \right) \vec{\nabla} \phi_i. \quad 3.$$

Equation 3 describes the forces in a system defined by a free energy functional,  $\mathcal{F} = \sum_i^N \mathcal{F}_i$ , defined below:

$$\begin{aligned} \mathcal{F}_i = & \frac{\gamma^i}{\lambda} \int d\vec{x} \left\{ 4\phi_i^2 (1 - \phi_i)^2 + \lambda^2 (\vec{\nabla} \phi_i)^2 \right\} \\ & + \mu \left( 1 - \frac{1}{V_0} \int d\vec{x} \phi_i^2 \right)^2 + \sum_{j \neq i} \frac{\kappa_{\text{cc}}}{\lambda^2} \int d\vec{x} \phi_i^2 \phi_j^2 \end{aligned}$$



$$\begin{aligned}
& + \sum_{j \neq i} \omega_{cc}^j \int d\vec{x} \vec{\nabla} \phi_i \cdot \vec{\nabla} \phi_j + \frac{\kappa_{cs}}{\lambda^2} \int d\vec{x} \phi_i^2 \phi_w^2 \\
& + \omega_{cs}^i \int d\vec{x} \vec{\nabla} \phi_i \cdot \vec{\nabla} \phi_w. \tag{4}
\end{aligned}$$

The first term in the free energy functional, defined by Equation 4, encapsulates the intrinsic energy of cell  $i$ . In this instance, this is achieved by a symmetric double-well potential that establishes a preference for two distinct phases, i.e., the inside and outside of a cell as well as a gradient term. It penalizes spatial variation in  $\phi_i$ , where the parameter  $\lambda$  sets the length scale associated with the diffusive interface. The second term in Equation 4 enforces a volume constraint, ensuring that the volume of cell  $i$  does not deviate significantly from the imposed volume,  $V_0 = (4/3)\pi R_0^3$ , where  $R_0$  is the initialized cell radius. The energy cost due to any deviation grows quadratically with strength  $\mu$ . The third term in Equation 4 specifies repulsion with strength  $\kappa_{cc}$  between cells  $i$  and  $j$  with a quadratic form based on overlapping phase fields (Figure 1a), making the energy cost more sensitive to the degree of overlap. In general, any positive even exponent suffices to avoid attraction due to very small negative phase-field values that may arise numerically. The fourth term in Equation 4 captures cell-cell adhesion interactions of strength  $\omega_{cc}^i$ . This term contributes only when the gradients of phase-fields  $i$  and  $j$  overlap spatiotemporally, given the gradients are only nonzero at the interface. This differs from the repulsion term (third term in Equation 4) that is based on the overlap of phase fields and not their gradients. The second to last and last terms have structures similar to those of the third and the fourth terms for cell-cell repulsion and adhesion but with different parameterizations for strength, i.e., cell-substrate

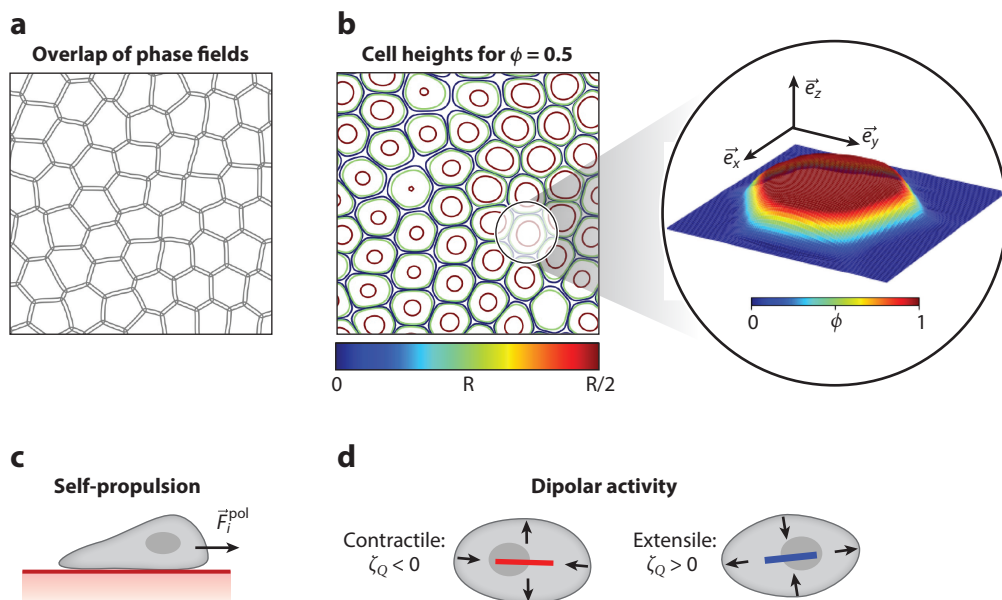


**Figure 1**

Multiphase-field model. (a) Visualization of overlapping phase fields for  $\phi_i = 0.1$ . (b) Visualization of cell heights and their fluctuations for a simulated three-dimensional monolayer. The inset plot demonstrates a single scalar phase field,  $\phi$ , in three dimensions. (c) Schematic representation of self-propulsive force,  $\vec{F}_i^{\text{pol}}$ . (d) Schematic representation of nematic active stresses for contractile and extensile systems. Red and blue lines represent the nematic director.

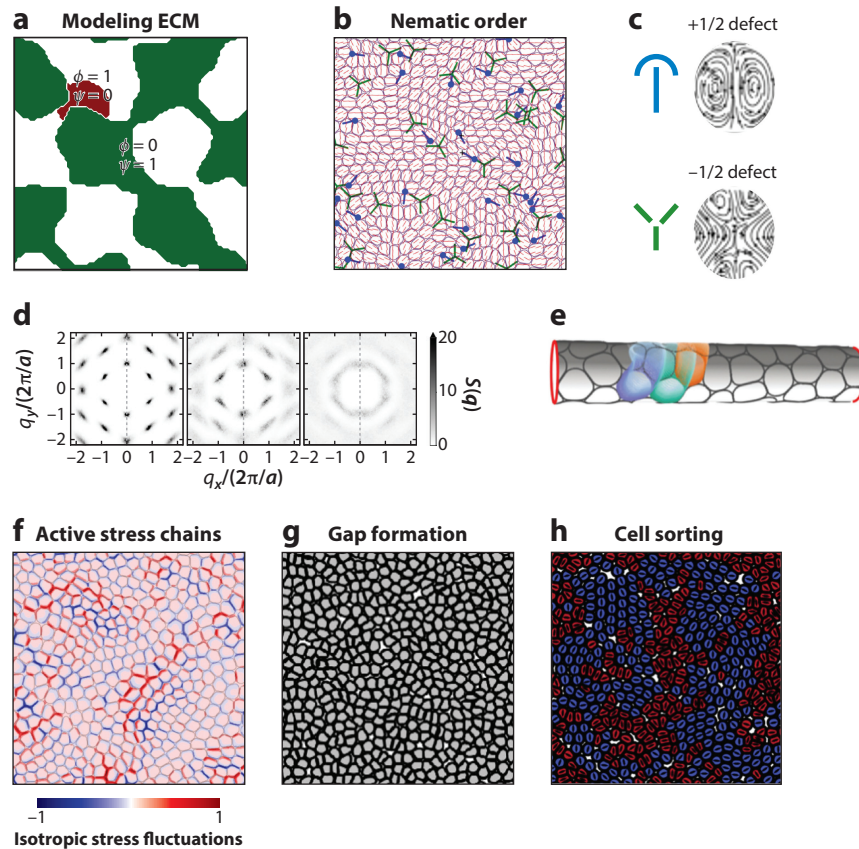


**Figure 2**

Multiphase-field models and physics of active matter. (a) Simulation setup in which one phase field ( $\phi$ ) defines the cell, whereas the other ( $\Psi$ ) defines the ECM. (b) A coarse-grained director field plotted on top of cell interfaces ( $\phi = 0.5$ ) with  $+1/2$  (filled circles with a line indicate orientation) and  $-1/2$  (three connected lines with threefold symmetry) indicate nematic defects. (c) Average flow fields around  $+1/2$  and  $-1/2$  topological defects. (d) Two-dimensional static structure factors for crystalline, hexatic, and isotropic liquid phases obtained from multiphase-field model simulations. (e) Snapshot of cell layer modeled on cylinder shape. (f) An example showing stress chains in an active monolayer. (g) Simulation snapshots of segregation in a 1:1 mixture of extensible (red) and contractile (blue) cells. (h) Snapshots of extensible cell monolayers demonstrating spontaneous formation of gaps. Panel b adapted from Reference 52 (CC BY 4.0). Panel c adapted with permission from Reference 47. Panel d adapted from Reference 88 (CC BY 4.0). Panel e adapted with permission from Reference 89. Panel f adapted from Reference 90 (CC BY 4.0). Panel g adapted with permission from Reference 91. Panel h adapted from Reference 39 (CC BY 4.0). Abbreviation: ECM, extracellular matrix.

repulsion,  $\kappa_{cs}$ , and cell–substrate adhesion,  $\omega_{cs}$ . In this 3D approach, cell heights emerge from collective interactions (Figure 1b), making it suitable to study inherently 3D biological processes such as cell extrusion. Furthermore,  $\phi_w$  is a static phase field that represents an arbitrarily defined 3D matrix, such as a dense fibrous network (51) (Figure 2a). This same construct can also account for a deformable matrix in which  $\phi_w = \phi_w(\vec{x}, t)$  evolves due to interactions with each cell and/or an externally imposed dynamics. This formulation can capture heterogeneity in interactions such as  $\gamma^i$  and  $\omega_{cc}^i$ , given the constraints imposed for stability are satisfied (see, e.g., 46). Furthermore,

the described multiphase-field approach is primarily concerned with physical interactions in active matter. However, such a framework can benefit from further expansion to include chemical activity (64, 65), typically captured by a Flory–Huggins-type free energy functional, coupling mechanics with (bio-)chemistry.

### 2.3. Nonequilibrium Behavior: Active Drive

Cell motility refers to the ability of a cell to move as it senses and reacts to its environment (66, 67). This is achieved mainly by local injection of energy supplied by adenosine triphosphate (ATP) fueling two processes that work together to generate self-propulsive forces: (a) actin polymerization that results in the formation of protrusions at the cell front and (b) myosin-driven contractility that pulls a cell's rear inward, enabling forward movement (68–70).

Such local injection of energy breaks time-reversal symmetry and detailed balance, giving rise to fascinating collective phenomena at length scales much greater than a single cell (71), including intricate and dynamic patterns critical for, e.g., embryogenesis. To this end, multicellular assemblies are a textbook example of active matter, defined as natural or synthetic systems composed of entities that dissipate energy to perform mechanical work on themselves and their environment (33, 72, 73). As such, living cells can be viewed as a particular instance of active matter with the ability to proliferate, differentiate, and mutate.

In this vein, activity is not limited to cell motility—it can also manifest at a length scale greater than an individual cell, e.g., due to proliferation (74, 75) and/or the poroelastic nature of cells and their surrounding environments; this breaks conservation of mass, volume, and number densities. In this review, we primarily focus on multiphase-field models with cell motility as the only source of activity. However, this modeling framework can indeed extend to account for activity due to expansion, such as cell division and/or poroelasticity.

In Equation 1, the nonconservative active forces  $\vec{F}_i^{\text{active}}$  are due to cell motility. A common physics-based model for cell motility uses the broken front–back symmetry from actin polarization. Generally, this manifests as a self-propulsion force that encodes a magnitude and a direction with some persistence to reflect directed motion (Figure 1c). Two frequently employed models are (a) active Ornstein–Uhlenbeck particles (AOUP) and (b) active Brownian particles (ABP) (76–78). A major distinction between the two models is that both magnitude and direction are stochastic in AOUPs, whereas ABPs follow a stochastic direction with a constant speed. For example, consider the following ABP-type model:

$$\vec{F}_i^{\text{pol}} = \alpha_i \vec{p}_i, \quad 5.$$

where  $\vec{p}_i = (\cos \theta_i, \sin \theta_i, 0)$ , a rank 1 tensor, is a front–back polarity vector attached to cell  $i$ , acting in-plane, and  $\alpha_i$  parameterizes the strength of polarity, akin to a constant velocity in the ABP model. This further necessitates a description for polarization dynamics, e.g., defined here as a stochastic process that aligns the polarity of the cell to the direction of the total passive interaction force,  $\vec{F}_i^{\text{passive}}$ :

$$\partial_t \theta_i = -\frac{1}{\tau_{\text{pol}}} \Delta \Theta_i + \sqrt{2D_r} \eta(t), \quad 6.$$

where  $\Delta \Theta_i$  is the angle between  $\vec{p}_i$  and  $\vec{F}_i^{\text{passive}}$ . Furthermore,  $\tau_{\text{pol}}$  sets the alignment timescale, and  $D_r$  represents rotational diffusivity, which is inversely related to persistent time.  $\eta(t)$  denotes standard Gaussian white noise with zero mean and unit variance, where  $\langle \eta(t) \eta(t') \rangle = \delta(t - t')$ . The model presented in Equations 5 and 6 agree well with the experimental characterization of collective motion of various cell cultures (79).



An important component of cell motility hinges on myosin contractility. This contractile active force is typically captured by nematic stress that is proportional to the nematic order parameter, a rank 2 tensor (32):

$$\sigma^{\text{nematic}} = \zeta_Q \sum_i \phi_i \mathbf{Q}_i, \quad 7.$$

where  $\zeta_Q$  represents the strength, contractile for  $\zeta_Q < 0$  and extensile for  $\zeta_Q > 0$ , and  $\mathbf{Q}_i = 2(\vec{n}_i \otimes \vec{n}_i - \frac{1}{2}\vec{n}_i^2)$ , where  $\mathbb{I}$  is rank 2 identity tensor. This active nematic stress introduces a dipolar force density along cells' interfaces (Figure 1d). The angle associated with  $\vec{n}_i$  can follow its own dynamics (39) or it can be set equal to cell polarity,  $\vec{n}_i = \vec{p}_i$ , e.g., ensuring contractile stresses act in the same direction as protrusion formation. The nematic order along the direction  $\vec{n}$  is head-tail symmetric, i.e.,  $\vec{n} \rightarrow -\vec{n}$ . This implies that polar entities with broken front-back symmetry can self-organize into nematic ordering if on average they align together while not pointing to a particular direction.

There is another rank 2 tensor construct for active drive that focuses on the generation of intercellular force through the adherent junctions (47). This approach utilizes a shape tensor,  $\mathbf{S}_i$ , to characterize shape anisotropy such that the direction associated with its largest eigenvalue captures the axis of elongation:

$$\sigma^{\text{shape}} = \zeta_S \sum_i \phi_i \mathbf{S}_i. \quad 8.$$

Here,  $\zeta_S$  denotes the strength of activity, with the same sign convention as  $\zeta_Q$ , and  $\mathbf{S}_i = -\int d\vec{x} \vec{\nabla} \phi^T \vec{\nabla} \phi$  is the traceless part of the negative of the structure tensor. Altogether, these active forces can be written as

$$\vec{F}_i^{\text{active}} = \int d\vec{x} (\sigma^{\text{nematic}} + \sigma^{\text{shape}}) \cdot \vec{\nabla} \phi_i + \vec{F}_i^{\text{pol}}. \quad 9.$$

The interplay of emerging order and the nature of active force generation remains an intense area of research (23, 35, 36, 80, 81), which we discuss further in Section 3.

Finally, using the definitions for active and passive forces (Equations 9 and 3, respectively) a rank 2 stress tensorial field can be constructed, providing access to in-plane and out-of-plane stress components. This is best achieved using a discrete stress definition consistent with those used in the granular physics and molecular dynamics communities (82, 83). Such a definition respects the discrete nature of a multiphase-field model. For passive stresses, another approach can be utilized based on Korteweg stresses for diffusive interfaces (84), commonly used in multiphase fluid mechanics for capillary stresses (85, 86) and most recently introduced in the context of a multiphase-field model (87).

### 3. MULTIPHASE-FIELD MODELS AND PHYSICS OF ACTIVE MATTER

From a physics perspective, the defining feature of a living matter is its nonequilibrium nature. In addition to providing significant biological insights, multiphase-field models provide a rich playground to explore ideas in nonequilibrium statistical physics, in particular systems in which constituent particles are capable of changing and adapting their shapes to the forces they experience. To this end, multiphase-field models have been instrumental in exploring the collective motion and the dynamic organization of deformable and shape-changing active particles. A number of studies have leveraged multiphase-field models to explore the emergence of order in active matter and its breakdown with significant consequences for living systems. This is discussed next, including exciting areas in which a multiphase-field approach promises novel physics insights.



### 3.1. Collective Self-Organization and Emergence of Order

Over the past two decades, extensive research has established a strong analogy between living matter—at multiple length scales—and active liquid crystals (92–94). This provides a rigorous theoretical framework to understand living matter and, in particular, dynamics of self-organization and collective behavior of cells and how it affects biological processes such as cancer metastasis (95). Liquid crystals are an intermediate phase of matter between solids and liquids, characterized by a short-range translational order and a quasi-long-range orientational order (96, 97). There are different phases of liquid crystals, generally named  $p$ -atic liquid crystals exhibiting  $p$ -fold rotational symmetry, i.e., symmetry with respect to rotations by  $2\pi/p$ . This forms the basis for the physics-based description of active force generation at the scale of a single cell and its interplay with the emergence of order at a much larger scale.

The order that emerges from self-organization in living cells governs the most fundamental biological processes such as development. Focusing on multicellular systems as opposed to sub-cellular ones, nematic order ( $p = 2$ ) and the associated half-integer topological defects have been reported in a number of cellular systems (98), including but not limited to Madin–Darby canine kidney (MDCK) cells (99, 100), human breast cancer cells (101), and neural progenitor stem cells (102). Similarly, multiphase-field models have shown the emergence of nematic order due to force generation mechanisms defined by rank 2 active stress tensors (39, 47) (Equations 7 and 8). Concurrently, the coemergence of nematic (Figure 2b) and hexatic orders from active polar forces, Equations 5 and 6, has been captured by a multiphase-field model (52). Furthermore, Armengol-Collado et al. (36) have demonstrated coexistence of both nematic and hexatic orders in confluent cell layers depending on the length scales of interest: two-fold nematic ( $p = 2$ ) is dominant at larger scales, whereas six-fold hexatic ( $p = 6$ ) is dominant at smaller length scales (Figure 2c). This is achieved by complementing in vitro experiments on confluent MDCK cells with multiphase-field and self-propelled Voronoi models. This hierarchical structure has also been recovered from a hydrodynamics description of confluent epithelial monolayers (103), hinting at the generality of this approach. Recent experiments complemented with vertex-based modeling show how correlated cell division can lead to the emergence of tetric ( $p = 4$ ) order (23). Viewing multicellular assemblies as multiscale  $p$ -atic active liquid crystals provides a powerful framework for understanding the dynamics of self-organization and collective behavior of cells with important implications for  $p$ -atic defect dynamics that is crucial to some of the most fundamental biological processes.

### 3.2. Collective Self-Organization and Breakdown of Order: Topological Defects

Topological defects refer to singularities that disrupt field symmetry. In living cells, they can be formed because of geometric frustration, boundary conditions, and/or activity responsible for driving the system away from thermodynamic equilibrium. One of the key features of active liquid crystalline systems is the continuous formation and annihilation of topological defects. The multiphase-field models with shape-determined activity (47) and nematic dipolar activity (39) have not only reproduced the dynamics of topological defects but also accurately captured the flow fields and stresses around the defects (Figure 2d). This holds for both extensile and contractile systems. Furthermore, Zhang et al. (104) incorporated polar forces that arise from cytoskeletal propulsion, observing a sharp transition from jammed to liquid states, as well as flocking.

Topological defects have been associated with various biological functions, ranging from extrusion events in a cell monolayer (99) to the development of limbs in animals such as *Hydra* (105). Addressing such problems and understanding the underlying physics require transitioning from 2D modeling approaches to 3D ones. For example, the possibility of large overlaps developing between the cells at the points of fivefold disclinations was predicted using a 2D multiphase-field

model (48), and a recent 3D multiphase-field model linked cell extrusions to both half-integer nematic defects and fivefold disclinations in the hexatic order, with the strength of this link regulated by force transmission across the monolayer (52). Indeed, some confluent cell layers such as MDCK cells seem to behave like multiscale  $p$ -atic liquid crystals (36). This concept requires a nuanced understanding of  $p$ -atic defect dynamics and its interplay with various biological processes. For example, a recent study links the unbinding of hexatic defects to the process of cell intercalation, providing a possible explanation for the extensile nature of *in vitro* epithelial layers (106) through a process analogous to the Kosterlitz–Thouless–Halperin–Nelson–Young (KTHNY) melting scenario (107). A follow-up study uses a multiphase-field model to explore this link further by focusing on the onset of collective cell migration and the 2D defect-mediated melting, contrasting melting transition in active matter against its passive counterpart (88) (Figure 2e). In this vein, the emergence of both nematic and hexatic orders in confluent/near confluent active monolayers are linked to cellular geometry informed by intercellular friction and motility (108).

The dynamics of topological defects is also informed by geometrical frustration with fascinating implications (109). To this end, the application of the multiphase-field model on curved surfaces (110) can help decipher the role of local curvature in disrupting the local order and its biological consequences (Figure 2f), which is often manifested through the local stress fields as discussed in the next section.

### 3.3. Active Stress Chains and Force Transmission

The spatiotemporal dynamics of mechanical stresses play an important but poorly understood role in gene expression (111), genomic damage and potential mutation (112), and dynamics of expanding populations (113) as well as cell differentiation (114). At the same time, the transition of mechanical information is a primary suspect for facilitating collective self-organization, on a length scale much greater than an individual cell, and crucial for development and regeneration (13, 115). A recent computational study investigated solid-like to liquid-like transition in active monolayers by focusing on active stress chains and emerging stress patterns (90) (Figure 2g). Mapping this transition onto the 2D random percolation universality class using two independent active drives revealed the short-range nature of stress correlation near this transition, providing a new context for understanding the nonequilibrium physics of active systems and its connections to glass, jamming, and 2D melting transitions. Recent research has shown that activity-induced annealing can lead to a ductile-to-brittle transition in amorphous solids, which parallels the behavior observed in biological tissues under mechanical stress (116). This insight is crucial for understanding how mechanical forces influence tissue integrity and failure. In Section 4, which focusses on biological physics, we thoroughly discuss the role of force transmission on biological processes such as the fate of an extruding cell and cell competition.

## 4. BIOLOGICAL PHYSICS OF CELLS: INTEGRATION OF EXPERIMENTS WITH MULTIPHASE-FIELD MODELING

Besides understanding the physical properties of active matter, multiphase-field models have demonstrated the ability to capture the emergence of various biological phenomena driven by the mechanical properties of cells. For instance, cancer cells are known to differ mechanically from healthy counterparts. By modeling a single cancer cell in a layer of normal cells, the 2D multiphase-field model demonstrated that elasticity mismatch alone is sufficient to significantly increase the motility of the cancer cell (46). Additionally, simulations of extensile monolayers can capture a spontaneous formation of gaps (Figure 2b)—a phenomenon observed in epithelial monolayers (117). Finally, it is possible to model mixtures of both active and passive phases,



hence, reproducing interactions between cells and their environment, such as extracellular matrix (ECM) (Figure 2a) (51) or blood vessels.

In this section, we focus on the role of multiphase-field models on the interdisciplinary advances in multicellular systems, starting from parameterization of 2D cell monolayers to 3D models of embryogenesis. We focus particularly on problems in which multiphase-field modeling has been combined and studied together with relevant biological experiments. To bridge these different scales, we first discuss the importance of quantitative parameterization before examining the emergent behaviors that arise from mechanical interactions.

#### 4.1. Quantitative Modeling: Model Parameters Informed by Experiments

The precise matching of physical model parameters to biological systems is an outstanding challenge. Existing cell-based models have qualitatively reproduced flow fields and mechanical stresses around topological defects (100), as well as captured the amplitude and period of collective oscillations in confined epithelial monolayers (79). Using the cell length, cell velocity, and force units from experiments, the simulation length, time, and force units can be mapped directly into the physical units of  $\delta L \sim 2 \mu\text{m}$ ,  $\delta t \sim 0.1 \text{ min}$ , and  $\delta F \sim 200 \text{ nN}$ , respectively (Table 1).

Beyond direct parameter extraction, a powerful approach is that of transforming model parameters into dimensionless groups using Buckingham's  $\pi$  theorem (118, 119) (Table 2). The results of sensitivity analyses of dimensionless parameters in both two dimensions (47, 79, 100) and three dimensions (62) showed that the ratio of active to elastic forces,  $(\zeta R_0)/\gamma$ , is the predominant factor in governing cell deformation. In the 3D formulation, the ratio of the cell–cell to cell–substrate adhesion,  $\omega_{cc}/\omega_{cs}$ , is an additional significant parameter that affects collective cell motion in monolayers (52). These results set the foundation for understanding how mechanical interactions translate into emergent collective behaviors.

#### 4.2. From Microscale to Macroscale

Mechanical interactions govern the collective behavior of tissues, impact protein distributions, and have been shown to induce various biological functions (57). When placed on a solid substrate, an

**Table 1** Mapping of model parameters to physical units<sup>a</sup>

Simulation parameter	Physical meaning	Numerical value	Mapping to physical units	Measured physical value
$R_0$	Initial cell radius	8	15 $\mu\text{m}$	10–20 $\mu\text{m}$ (62)
$\gamma$	Cortex tension	0.008–0.016	800–1,600 pN/ $\mu\text{m}$	1,000–2,000 pN/ $\mu\text{m}$ (120, 121)
$\xi$	Friction coefficient	1	600 nN · s/ $\mu\text{m}$	$O(10^2)$ nN · s/ $\mu\text{m}$ (122, 123)
$\omega_{cc}$	Cell–cell adhesion force	0.006–0.012	12–24 nN	$O(10^1–10^2)$ nN (124)
$\omega_{cs}$	Cell–substrate adhesion force	0.001–0.002	2–4 nN	$O(10^1–10^2)$ nN (125, 126)
$\zeta$	Active stress	0.00001–0.001	0.5–50 Pa	$O(10^0–10^1)$ Pa (62)
$\tau_{\text{pol}}$	Cell polarity alignment time	200	20 min	$O(10^1)$ min (127)
$\alpha$	Single cell traction magnitude	0.05	10 nN	1–30 nN (128)
$\kappa_{cc}$	Cell–cell repulsion force	0.5	— <sup>b</sup>	—
$\kappa_{cs}$	Cell–substrate repulsion force	0.15	—	—
$\mu$	Stiffness of volume constraint	45	—	—
$\lambda$	Width of diffuse interface	1.5	—	—

<sup>a</sup>Note that in References 122 and 123, the friction coefficient is mapped by using Pa units for force, giving friction dimensions of nN · s/ $\mu\text{m}^3$  and is here converted to nN · s/ $\mu\text{m}$  using the cell size as the relevant length scale. Table adapted from Reference 62.

<sup>b</sup>“—” indicates that mapping to physical units is nonapplicable, because the parameter is model specific, and no experimental measurement is available.



**Table 2 Dimensionless model parameters and their physical interpretation<sup>a</sup>**

Dimensionless parameter	Physical interpretation	Sensitivity analyses
$\lambda/R_0$	Diffuse interface width compared to cell radius	Not sensitive: the width of the diffuse interface is set smaller than the cell radius ( $\lambda/R_0 \ll 1$ )
$\kappa R_0^2/\mu$	Cell-cell overlap to compressibility ratio	Not sensitive: only needed for keeping cell integrity and avoiding overlaps between phase fields
$\kappa_{cc}/\kappa_{cs}$	Cell-cell to cell-substrate repulsion energy ratio	Not sensitive: only needed to avoid overlap between phase fields representing cells and substrate
$\omega_{cc}/\omega_{cs}$	Cell-cell to cell-substrate adhesion energy ratio	One of the main control parameters
$\xi R_0/\gamma$	Contractility to stiffness ratio	One of the main control parameters
$\alpha\tau_{\text{pol}}/(\xi R_0)$	Ratio of realignment to directed motion time	Not sensitive: drives flocking behavior

<sup>a</sup>Table adapted from Reference 62.

epithelial cell exerts contractile forces—a pair of equal and opposite forces acting inward along the cellular axis. However, at the collective cell level, the monolayers yield extensile behavior, as observed from the flow fields and stress patterns around topological defects (99, 102, 129).

This puzzling difference between micro- and macroscale properties of cell monolayers has been explained using a 2D multiphase-field model, which simultaneously accounts for the properties of single cells and yields the resulting collective dynamics. The model accurately captured isotropic stresses around topological defects (Figure 3a) and predicted that the reduction in the strength of cell-cell interactions leads to an increase in cell–substrate interactions, which results in extensile nematic dynamics (100). This proposed mechanism was confirmed in experiments showing an increase in the strength of cell–substrate adhesion, affirming the emergence of intercellular extensile stresses through laser ablation experiments (100).

A complementary explanation was proposed by Zhang et al. (130), who demonstrated that fluctuations in phase-field models, rather than mean-field interactions alone, can also drive the observed extensile behavior. This highlights the need for a more comprehensive approach that integrates both deterministic and stochastic contributions to multiphase-field dynamics.

#### 4.3. Experimentally Informed Modeling of Collective Cell Migration in Two Dimensions

Collective cell migration *in vivo* is a complex and dynamic process essential for wound healing, embryogenesis, and cancer invasion (134). One aspect of this complexity is the influence of confinement and environmental interactions, which shape the collective and single-cell migration strategies observed in biological systems. Multiphase-field models have provided powerful tools to study these constraints, successfully replicating the dissociation of clusters from collectively invading cancer cells in confined geometries (131). By explicitly linking self-propulsion strength to chemical gradients and geometric confinement, such models have demonstrated that a solid-to-liquid transition along with the presence of leader cells exhibiting enhanced motility are both necessary for rupture events to occur (Figure 3b). Additionally, they have revealed how parameters such as channel width and cell–cell adhesion influence the likelihood of cluster rupture, shedding light on migration strategies across diverse microenvironments.

Beyond confinement effects, recent studies have emphasized another layer of complexity in cell migration—interactions with self-deposited traces. Experimental work has shown that migrating cells can modify their own microenvironment by secreting ECM components or depleting substrate adhesiveness, thereby altering the effective landscape for subsequent migration (135).



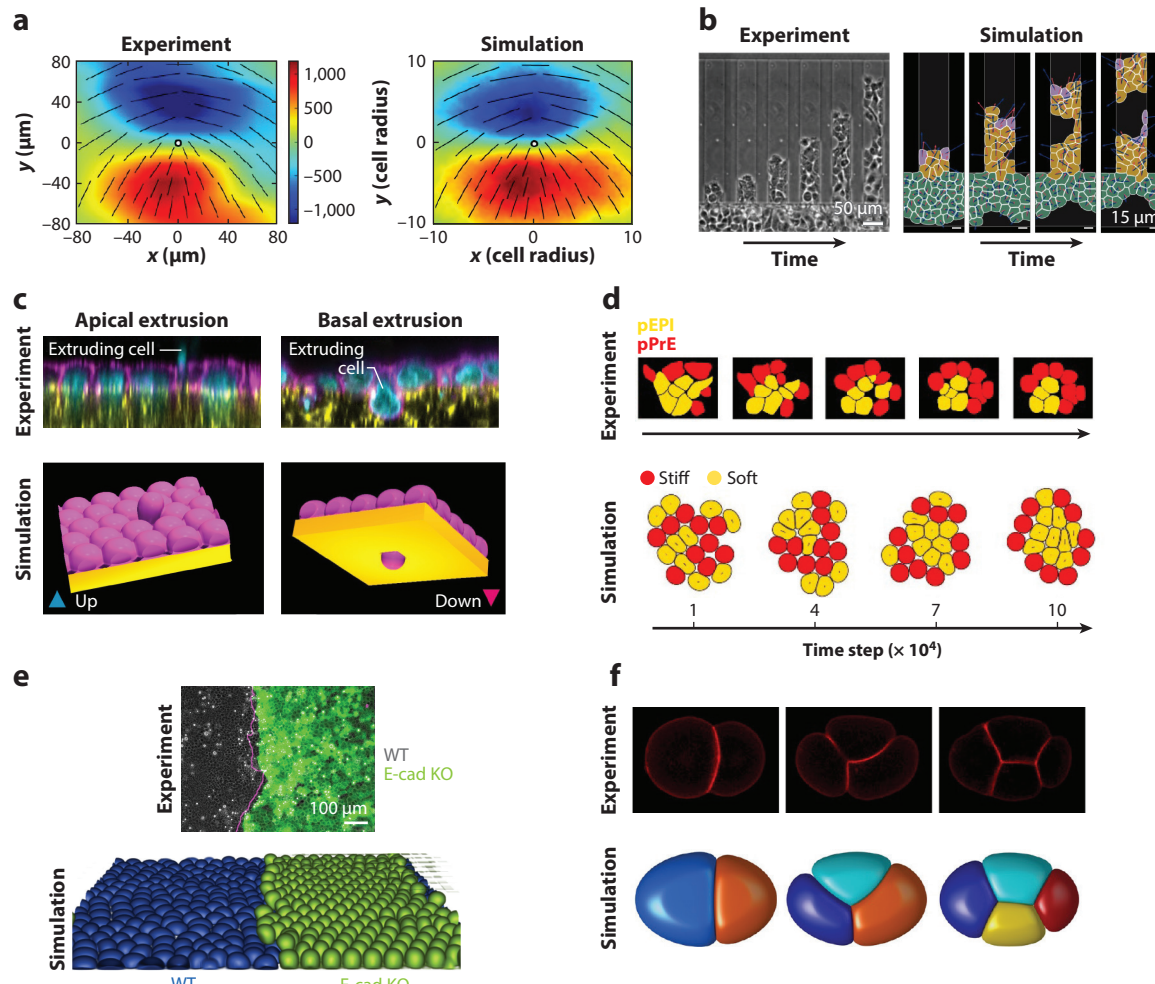


Figure 3

Biological physics of cells. Integration of experiments with multiphase-field modeling. (a) Average isotropic stress around a  $+1/2$  defect obtained from experiments on MDCK E-cad KO cells (left) and simulations (right). (b, left) Phase contrast snapshots of invading human A431 epidermoid carcinoma cells confined in 50- $\mu\text{m}$  microchannels. (b, right) Evolution of rupture for simulations of cells in microchannels with 50- $\mu\text{m}$  width. (c, top) Orthogonal view of immunostaining of MDCK WT (left) and MDCK E-cad KO (right) monolayers grown on two-dimensional type-I collagen gels, actin (magenta), collagen (yellow), and nuclei (cyan). Arrows indicate an extruding cell. (c, bottom) Snapshots from simulations demonstrating apical and basal extrusions by varying activity and cell-cell adhesion. (d, top) Time-series snapshots of experimental segregation of pEPI cells in yellow, pPrE cells in red. (d, bottom) Simulation snapshots of the segregation of a 20-cell aggregate of soft (yellow) and stiff (red) cells. (e) Mechanical cell competition between two colliding assays of WT and E-cad KO cells, displaying the cell type and location of extrusions [white spots in experimental image frame (top) and simulations (bottom)]. (f) Comparison between *in vivo* fluorescence images and *ab initio* simulations of *Caenorhabditis elegans* embryonic morphologies from 2- to 4-cell stages. Panel a adapted with permission from Reference 100. Panel b adapted from Reference 131 (CC BY 4.0). Panel c adapted with permission from Reference 62. Panel d adapted with permission from Reference 132. Panel e adapted with permission from Reference 133. Panel f adapted from Reference 53 (CC BY 4.0). Abbreviations: E-cad, E-cadherin; KO, knockout; MDCK, Madin-Darby canine kidney; pEPI, epiblast cell; pPrE, primitive endoderm cell; WT, wild type.

Multiphase-field models incorporating such feedback mechanisms reveal emergent behaviors in which cells exhibit persistent or oscillatory motion in response to their own tracks (136), highlighting a form of self-guided navigation that can either enhance or inhibit migration efficiency. These findings suggest that cell motility is dictated by not only external constraints but also the dynamic remodeling of the environment through cellular activity, underscoring the importance of coupling biochemical and mechanical interactions in predictive models of migration.

By integrating insights from both confinement-induced migration and self-trace interactions, multiphase-field models provide a mechanistic framework to explore emergent migration behaviors. Such approaches offer a deeper understanding of how cells navigate complex landscapes, with implications for tissue development, immune responses, and metastatic invasion.

#### 4.4. From Two Dimensions to Three Dimensions: Mechanical Imprints of Live Versus Dead Cell Elimination

Even though in appropriate limits cell monolayers can be approximated as a 2D problem (87), there are various biological phenomena that require consideration of the third dimension. This is particularly relevant in cell extrusion—the process by which cells are removed from a monolayer.

Cells can be extruded either live or dead. Determining how the fate of an extruding cell is decided remains a major question in biology with significant implications for tissue and organ development under both normal and pathological conditions. In a combined experimental and multiphase-field modeling approach, it was shown that weakening cell–cell contacts, effectively altering the force transmission capability of cells, affects the local stress patterns near an extruding cell (62). The multiphase-field model was able to capture the distributions for the local stress fields and their temporal evolutions for both normal and transformed cell types. These quantitative insights revealed how the intensity and duration of local stress fields shape the survival or death of an extruding cell.

Furthermore, the same multiphase-field model was employed to predict the direction of cell extrusion, apical versus basal, on a soft porous collagen substrate. The extended model incorporated irregular environments through an additional phase field representing a deformable ECM. The model predicted that cells with lower cell–cell adhesion and higher contractility preferentially extrude basally, consistent with experiments (Figure 3c). These insights have since been extended to 3D cysts in matrigel, reinforcing the universality of mechanical cues governing the fate of an extruding cell.

#### 4.5. Heterogeneous Cell Populations

Biological tissues are not perfectly uniform in terms of cell mechanical properties and often exhibit heterogeneity, in which cells with different mechanical properties coexist. One of the advantages of multiphase-field models is their ability to incorporate such heterogeneity and isolate the effects of specific mechanical parameters.

The cell-sorting phenomenon has been of particular interest (91) (Figure 2i). A 2D multiphase-field model demonstrated that differences in elasticity alone can drive autonomous segregation, in which softer cells, which collectively exhibit fluid-like behavior, become surrounded by stiffer cells, which collectively exhibit solid-like behavior (132). This mechanism explains the segregation of primitive endoderm (pPrE) and epiblast (pEPI) cells observed in mouse embryonic stem cell experiments (Figure 3d).

Additional phase-field studies on cell sorting, such as those conducted in References 91 and 100, have highlighted the role of adhesion heterogeneity and active forces in determining sorting outcomes. In particular, recent research has demonstrated that mixtures of cells exhibiting



distinct dipolar activities—either extensile or contractile—can spontaneously segregate into elongated domains. This segregation is driven by differences in cellular diffusivity, akin to the behavior of Brownian particles connected to thermostats at varying temperatures. Notably, this mechanism operates independent of traditional thermodynamic factors, underscoring the significance of active forces in cellular self-organization. Additionally, phase-field modeling combined with experiments on MDCK cells demonstrated how the interplay between cell–substrate interactions and active stresses regulate sorting of extensile and contractile cells when they adhere strongly to the substrate (100).

The emergence of new physics through multiphase-field modeling has been particularly enlightening. These models have revealed that the interplay between active forces and mechanical properties can lead to novel segregation patterns, such as the formation of extensile and contractile domains. This insight is crucial for understanding how cells self-organize in a tissue, providing a more comprehensive framework for studying developmental processes and disease progression.

Overall, these modeling predictions and comparison with experiments (100) highlight the distinct mechanisms of phase separation driven by differences in cellular activity compared to traditional differential adhesion or line tension models. While initial studies focused on cadherin-mediated surface tension as a primary driver of tissue segregation (137), it is now evident that intercellular adhesion is not the sole factor. Theoretical models suggest that a combination of cell surface tension and contractility can also drive cell sorting (138). Although differential adhesion and line tension may still play a role, the results emphasize the critical importance of cell–substrate interactions and intracellular stresses in regulating cell sorting within strongly adherent cellular monolayers (100, 139). Hence, incorporating cell heterogeneity at various levels could provide a more comprehensive framework for understanding self-organization in developing tissues.

#### 4.6. Mechanical Competition in Heterogeneous Cell Populations

Although competition within heterogeneous cell populations can dictate survival dynamics at the tissue level, the spatial organization of these populations is also influenced by external constraints and geometric confinement. Cells in heterogeneous populations not only coexist and segregate but also compete with each other for space and nutrients. Cell competition is crucial for not only maintaining homeostasis and fighting pathogens but also the progression of diseases, such as cancer (60). By modeling two distinct cell types (Figure 3e) and directly measuring the forces the cells exhibit on each other, the multiphase-field model demonstrated the emergence of in-plane stress fluctuations at the interface of two competing cell populations (133). This is a crucial feature in understanding the outcome of mechanical cell competition: The cell type with a stronger cell–cell adhesion strength can more effectively transmit these interfacial stress fluctuations away from the frontline cells near the interface onto the bulk. This translates into a competitive advantage relative to cells with a weaker cell–cell adhesion strength and, hence, stress transmission capability, where in-plane stress fluctuations become localized and induce out-of-plane stresses—reminiscent of the Poisson effect in elasticity—which can lead to a higher probability for cell elimination. Importantly, these predictions were compared with and confirmed by direct experimental measurements of forces in between competing cell types (133).

The multiphase-field modeling approach is pivotal in revealing the intricate physics of mechanical competition. It allows for the detailed simulation of differential force transmission capabilities between cell types, which play a crucial role in determining the outcome of cell competition. Cells with stronger intercellular adhesion exhibit higher resistance to elimination due to their ability to efficiently transmit forces to neighboring cells, thereby maintaining tissue integrity and boundaries. This efficient force transmission results in increased mechanical activity at the interface



of competing cell populations, characterized by large stress fluctuations. These fluctuations can induce upward forces, leading to the elimination of cells with weaker adhesion properties.

Furthermore, the multiphase-field model underscores the importance of mechanical forces in maintaining tissue homeostasis and preventing pathological conditions such as tumorigenesis. The ability of cells to mechanically outcompete each other through directed migration, crowding, and differences in growth rates underscores the complex interplay between biochemical and mechanical factors in cell competition. Understanding these mechanisms through multiphase-field modeling provides valuable insights into the development of therapeutic strategies aimed at modulating cell competition to treat diseases characterized by abnormal cell proliferation and invasion.

#### 4.7. Confined Cellular Systems in Three Dimensions

Extending beyond competition within planar tissues, the role of confinement becomes particularly relevant in 3D contexts, where cells are influenced by not only their neighbors but also surrounding structural constraints. In many biological conditions, cells do not simply exist as monolayers. Instead, they form 3D structures that are confined and may change over time owing to proliferation or external environmental factors. This is particularly important during morphogenesis, when an organism starts as a single cell, and undergoes division and self-organization—all dictated by genetic factors, as well as physical forces (140). The phase-field formalism allows for the prescription of various geometries and, with proper parameterization using experimental data, can be suitably adapted for unraveling the physics behind the early stages of morphogenesis. By extracting accurate geometrical constraints and relevant parameter values from experimental 3D time-lapse cellular *in vivo* imaging of developing *Caenorhabditis elegans*, the model can precisely reproduce the time evolution of the location and shapes of every cell during the morphogenetic transformation from 1- to 4-cell stages (Figure 3f) (141). The model predicts how physical factors, such as cell division timing, cell division orientation, and cell–cell attraction matrix, govern robust morphological evolution at 6-, 7-, and 8-cell stages.

The examples discussed illustrate the versatility of multiphase-field models in capturing key biophysical processes across different scales in biological tissues. These models have proven essential in elucidating cell migration, collective behavior, extrusion dynamics, and mechanical competition. However, significant challenges remain, which we discuss in the next section.

### 5. CHALLENGES AND FUTURE DIRECTIONS

Despite the significant progress made, several challenges remain in the development and application of multiphase-field models. One major challenge is the accurate representation of the complex mechanical and biochemical interactions within tissues. While current models capture key mechanical properties at a single-cell level, many features have yet to be incorporated.

Mechanotransduction, the process by which cells convert mechanical stimuli into biochemical signals, is a critical area for future research. Phase-field models can be extended to include mechanotransduction pathways, allowing for a more comprehensive understanding of how mechanical forces influence cell behavior and tissue development (143). This will involve integrating mechanical feedback mechanisms and signaling pathways into the models to simulate how cells sense and respond to their mechanical environment.

Modeling the mechanical interaction between the cell nucleus and the active cytoskeleton is another important direction. The nucleus plays a crucial role in cellular mechanics, and its interaction with the cytoskeleton affects various cellular processes, including migration and differentiation (144–146). Incorporating the mechanical properties of the nucleus and its interactions



with the cytoskeleton into phase-field models will provide deeper insights into the role of nucleus mechanics in cell behavior.

Using phase-field models to understand and explore emergent collective modes and long-range ordering of cells is another exciting direction. Cells in tissues exhibit collective behaviors that arise from their interactions and mechanical properties. Phase-field models can be used to study these emergent behaviors and understand the principles that govern long-range ordering in cell collectives (147). In this vein, another promising direction is the coupling of multiphase-field models with hydrodynamic flows. Recent research has revealed the importance of water transport, viscosity, and flow in cellular processes. Water and hydraulic pressure play essential roles in cell shape changes, motility, and tissue function, generating significant mechanical forces (148). Coupling multiphase-field models with hydrodynamic models will allow for a more accurate representation of these processes, providing insights into how fluid dynamics influence cell behavior and tissue mechanics. This approach can help elucidate the role of hydraulic resistance and external hydraulic pressures in cell polarization and motility, as well as the impact of fluid-structure interactions on cellular and tissue dynamics (149). In addition, extending multiphase-field models to capture interstitial fluid transport and viscoelastic properties of the ECM will enhance their applicability to realistic tissue environments, further bridging the gap between simulations and experimental observations.

An important future challenge is the explicit incorporation of different types of fluctuations—thermal, active, and biochemical—into phase-field models. Although thermal fluctuations play a minor role in large-scale tissue mechanics, they remain relevant at the subcellular level. Active fluctuations, arising from cytoskeletal remodeling and stochastic motor activity, introduce nonequilibrium noise that significantly affects cellular dynamics, phase separation, and collective behavior. Incorporating such fluctuations into multiphase-field models is crucial for understanding how cell-to-cell variability, stochastic biochemical signaling, and active force generation contribute to emergent tissue properties. Furthermore, biochemical noise in reaction-diffusion systems can lead to spatial heterogeneities and stochastic transitions in cell fate decisions, requiring models to integrate stochasticity in both mechanical and biochemical fields. Addressing these challenges will be key to improving the predictive power of phase-field models and their ability to capture the full complexity of living tissues.

Capturing shape changes of cells in collectives is another critical area for future research. Cells in tissues undergo complex shape changes during migration, division, and differentiation. Extending phase-field models to accurately simulate these shape changes, including cell proliferation as demonstrated in **Figure 4a**, will provide valuable insights into the mechanics of tissue morphogenesis and the factors that drive these shape changes (151). Advanced modeling techniques, such as the cellular Potts model, have shown promise in accurately predicting 3D cell shapes in structured environments (151).

Volume fluctuations and the compressibility of cells in collectives are also important aspects to consider. Cells in tissues exhibit volume changes due to various factors, including osmotic pressure and mechanical forces, as clearly shown in the image of MDCK cell monolayers in **Figure 4b**. Modeling these volume fluctuations and their impact on collective cell behavior will enhance our understanding of tissue dynamics and the mechanical properties of cell collectives (152). Recent studies have shown that cell volume fluctuations can significantly influence collective migration and tissue organization, highlighting the need for more detailed models that capture these dynamics (153).

Extending phase-field models to account for complex 3D structures is crucial, as even 2D monolayers may exhibit heterogeneities in the  $z$  direction, as shown by the dome formation in MDCK cell monolayers (**Figure 4c**). Furthermore, the modeling of organoids and spheroids



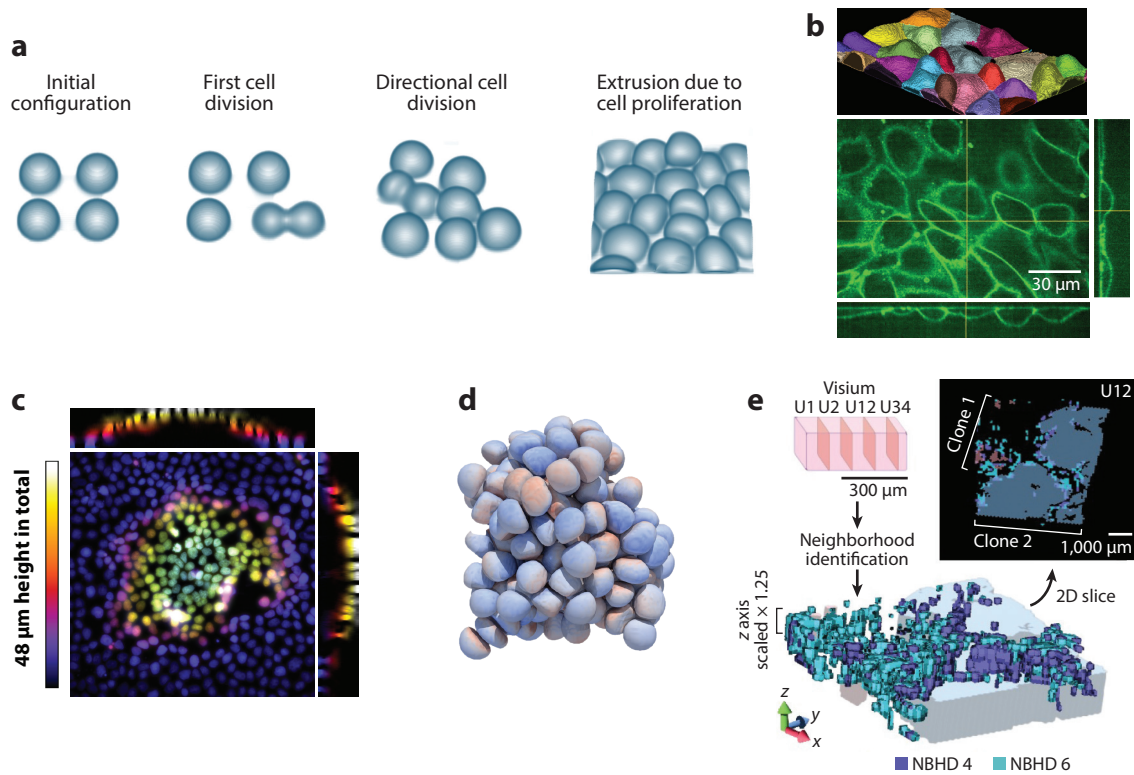


**Figure 4**

Challenges and future directions for multiphase-field modeling of biological tissues. (a) Snapshots of a simulation demonstrating proliferating cells in a 3D multiphase-field model. (b, *bottom*) Orthoviews (*xy*, *xz*, *yz*) of MDCK cells that are stained with a membrane dye. (b, *top*) 3D segmentation of the cell surface performed using *Cellpose*. (c) MDCK E-cadherin-RFP cells that have been cultured on a glass coated with fibronectin for about 2 days and then fixed and dyed with Hoechst. (d) Snapshot of a multiphase-field simulation of a 3D cell cluster. (e) Reconstructed 3D neighborhood volumes of a metastasis tissue sample. Images in panel *b, top*, provided by Valeria Grudtsyna. Images in panel *c* provided by Valeria Grudtsyna. Panel *d* adapted with permission from Reference 150; image provided by Haochun Sun. Panel *e* adapted from Reference 142 (CC BY 4.0). Abbreviations: 2D, two-dimensional; 3D, three-dimensional; MDCK, Madin–Darby canine kidney; NBHD, neighborhood; RFP, red fluorescent protein.

within a multiphase-field framework is a promising direction for understanding tissue and organ development, as these systems mimic the structure and function of tissues and organs. Phase-field models can be used to simulate the growth and development of these systems (Figure 4*d*), providing insights into the factors that influence their morphology and function (154). Recent studies have demonstrated the potential of phase-field models to predict organoid morphology and understand the mechanical factors that drive their self-organization (154). However, a comprehensive framework should also account for chemical signaling and reaction-diffusion processes that regulate organoid development. This can be achieved by coupling mechanics with biochemical activity, such as through a Flory–Huggins-type free energy functional, to model phase separation and cellular differentiation (64, 65). Expanding phase-field models to integrate such chemical interactions will enhance our understanding of how biochemical gradients and mechanical forces coordinate organoid growth, patterning, and fate decisions.

Furthermore, recent advances in the 3D imaging of patient tumors and identifying cancer cell subpopulations (Figure 4*e*) pave the way toward understanding the interplay between

the mechanical properties of cells and the tumor microenvironment. Despite their success in capturing the collective organization of cells, multiphase-field models face several challenges in fully representing the complexity of tumor dynamics. One key challenge is incorporating the heterogeneous mechanical properties of tumors, in which stiffness gradients and local deformations influence cell migration and invasion. Additionally, improving the resolution and computational efficiency of these models remains an ongoing challenge, particularly when simulating large-scale tumors with intricate mechanical interactions. Another crucial direction is the integration of poroelastic effects to account for the role of interstitial flows and pressure gradients, which significantly impact tumor expansion and cell motility. Finally, advancing these models to include the dynamic remodeling of the ECM and its feedback on tumor progression will be essential for capturing the evolving mechanical landscape of growing tumors. Addressing these challenges will enhance the predictive power of multiphase-field models and enable more precise insights into tumor mechanics and morphology.

Overall, multiphase-field models continue to be a cornerstone of biological and physical research, offering unparalleled insights into the dynamic and complex nature of cellular, tissue, and physical systems. The integration of diverse biological processes and mechanical interactions into these models has enabled researchers to explore the fundamental principles governing tissue dynamics and development, paving the way for new discoveries and advancements in the field. Future expansions of these models, incorporating biochemical signaling, hydrodynamic interactions, and tissue-specific regulatory mechanisms, will be essential for developing a more unified and predictive framework for biological morphogenesis. Additionally, systematically incorporating stochastic effects and active fluctuations into these models will provide a deeper understanding of robustness in developmental processes and the role of noise in cellular decision-making. The application of physical principles in these models not only enhances our understanding of biological systems but also drives innovation in computational methods, leading to more accurate and predictive simulations of cellular and tissue dynamics.

## DISCLOSURE STATEMENT

The authors are not aware of any affiliations, memberships, funding, or financial holdings that might be perceived as affecting the objectivity of this review.

## ACKNOWLEDGMENTS

We apologize to our colleagues whose valuable work could not be cited in this review because of focusing on recent advancements on only multiphase-field models of cell layers.

A.A. acknowledges support from the European Union's Horizon Europe research and innovation program under the Marie Skłodowska-Curie grant agreement 101063870 (TopCellComm). A.D. acknowledges funding from the Novo Nordisk Foundation (grant NNF18SA0035142 and NERD grant NNF21OC0068687), Villum Fonden grant 29476, and the European Union via the European Research Council-Starting Grant PhysCoMeT grant 101041418.

## LITERATURE CITED

1. Darwin C. 1859. *On the Origin of Species by Means of Natural Selection, or the Preservation of Favoured Races in the Struggle for Life*. John Murray
2. Maskarinec SA, Franck C, Tirrell DA, Ravichandran G. 2009. *PNAS* 106(52):22108–13
3. Nier V, Jain S, Lim CT, Ishihara S, Ladoux B, Marcq P. 2016. *Biophys. J.* 110(7):1625–35
4. Mongera A, Rowghanian P, Gustafson HJ, Shelton E, Kealhofer DA, et al. 2018. *Nature* 561(7723):401–5
5. Latorre E, Kale S, Casares L, Gómez-González M, Uroz M, et al. 2018. *Nature* 563(7730):203–8



6. Mo CK, Liu J, Chen S, Storrs E, Targino da Costa ALN, et al. 2024. *Nature* 634(8036):1178–86
7. Aranson IS, ed. 2015. *Physical Models of Cell Motility*. Springer International Publishing. 1st ed.
8. Petridou NI, Heisenberg CP. 2019. *EMBO J.* 38(20):e102497
9. Tetley RJ, Staddon MF, Heller D, Hoppe A, Banerjee S, Mao Y. 2019. *Nat. Phys.* 15(11):1195–203
10. Jain A, Ulman V, Mukherjee A, Prakash M, Cuenca MB, et al. 2020. *Nat. Commun.* 11(1):5604
11. Grosser S, Lippoldt J, Oswald L, Merkel M, Sussman DM, et al. 2021. *Phys. Rev. X* 11(1):011033
12. Blauth E, Kubitschke H, Gottheil P, Grosser S, Käs JA. 2021. *Front. Phys.* 9:666709
13. Vining KH, Mooney DJ. 2017. *Nat. Rev. Mol. Cell Biol.* 18(12):728–42
14. Chiou K, Collins EMS. 2018. *Dev. Biol.* 433(2):155–65
15. Tse JM, Cheng G, Tyrrell JA, Wilcox-Adelman SA, Boucher Y, et al. 2011. *PNAS* 109(3):911–16
16. Amos SE, Choi YS. 2021. *Front. Bioeng. Biotechnol.* 9:625859
17. Camley BA, Rappel WJ. 2017. *J. Phys. D: Appl. Phys.* 50(11):113002
18. Moure A, Gomez H. 2019. *Arch. Comput. Methods Eng.* 28(2):311–44
19. Alert R, Trepat X. 2020. *Annu. Rev. Condens. Matter Phys.* 11:77–101
20. Farhadifar R, Röper JC, Aigouy B, Eaton S, Jülicher F. 2007. *Curr. Biol.* 17(24):2095–104
21. Bi D, Yang X, Marchetti MC, Manning ML. 2016. *Phys. Rev. X* 6(2):021011
22. Park JA, Kim JH, Bi D, Mitchel JA, Qazvini NT, et al. 2015. *Nat. Mater.* 14(10):1040–48
23. Cislo DJ, Yang F, Qin H, Pavlopoulos A, Bowick MJ, Streichen SJ. 2023. *Nat. Phys.* 19(8):1201–10
24. Okuda S, Inoue Y, Adachi T. 2015. *Biophys. Physicobiol.* 12(0):13–20
25. Rozman J, Yeomans JM. 2024. *Phys. Rev. Lett.* 133(24):248401
26. Henkes S, Fily Y, Marchetti MC. 2011. *Phys. Rev. E* 84(4):040301
27. Basan M, Elgeti J, Hannezo E, Rappel WJ, Levine H. 2013. *PNAS* 110(7):2452–59
28. Smeets B, Alert R, Pešek J, Pagonabarraga I, Ramon H, Vincent R. 2016. *PNAS* 113(51):14621–26
29. Graner F, Glazier JA. 1992. *Phys. Rev. Lett.* 69(13):2013–16
30. Toner J, Tu Y. 1995. *Phys. Rev. Lett.* 75(23):4326–29
31. Toner J, Tu Y. 1998. *Phys. Rev. E* 58(4):4828–58
32. Simha RA, Ramaswamy S. 2002. *Phys. Rev. Lett.* 89(5):058101
33. Marchetti MC, Joanny JF, Ramaswamy S, Liverpool TB, Prost J, et al. 2013. *Rev. Mod. Phys.* 85(3):1143–89
34. Doostmohammadi A, Ignés-Mullol J, Yeomans JM, Sagués F. 2018. *Nat. Commun.* 9:3246
35. Maitra A, Lenz M, Voituriez R. 2020. *Phys. Rev. Lett.* 125(23):238005
36. Armengol-Collado JM, Carenza LN, Eckert J, Krommydas D, Giomi L. 2023. *Nat. Phys.* 19(12):1773–79
37. Löber J, Ziebert F, Aranson IS. 2015. *Sci. Rep.* 5(1):9172
38. Marth W, Voigt A. 2016. *Interface Focus* 6(5):20160037
39. Ardaševa A, Mueller R, Doostmohammadi A. 2022. *Soft Matter* 18(25):4737–46
40. Biben T, Misbah C. 2003. *Phys. Rev. E* 67(3):031908
41. Lowengrub JS, Rätz A, Voigt A. 2009. *Phys. Rev. E* 79(3):031926
42. Kockelkoren J, Levine H, Rappel WJ. 2003. *Phys. Rev. E* 68(3):037702
43. Shao D, Rappel WJ, Levine H. 2010. *Phys. Rev. Lett.* 105(10):108104
44. Ziebert F, Swaminathan S, Aranson IS. 2011. *J. R. Soc. Interface* 9(70):1084–92
45. Moure A, Gomez H. 2017. *Comput. Methods Appl. Mech. Eng.* 320:162–97
46. Palmieri B, Bresler Y, Wirtz D, Grant M. 2015. *Sci. Rep.* 5:11745
47. Mueller R, Yeomans JM, Doostmohammadi A. 2019. *Phys. Rev. Lett.* 122(4):048004
48. Loewe B, Chiang M, Marenduzzo D, Marchetti MC. 2020. *Phys. Rev. Lett.* 125(3):038003
49. Wenzel D, Voigt A. 2021. *Phys. Rev. E* 104(5):054410
50. Nonomura M. 2012. *PLOS ONE* 7(4):e33501
51. Moreira-Soares M, Cunha SP, Bordin JR, Travasso RDM. 2020. *J. Phys. Condens. Matter* 32(31):314001
52. Monfared S, Ravichandran G, Andrade J, Doostmohammadi A. 2023. *eLife* 12:e82435
53. Kuang X, Guan G, Tang C, Zhang L. 2023. *npj Syst. Biol. Appl.* 9(1):6
54. Chan CJ, Costanzo M, Ruiz-Herrero T, Mönke G, Petrie RJ, et al. 2019. *Nature* 571(7763):112–16
55. Nelson CM. 2022. *Annu. Rev. Biomed. Eng.* 24:307–22
56. Kuipers D, Mehanic A, Kajita M, Peter L, Fujita Y, et al. 2014. *J. Cell Sci.* 127(Pt 6):1229–41

57. Ladoux B, Mège RM. 2017. *Nat. Rev. Mol. Cell Biol.* 18(12):743–57
58. Khalil AA, Ilina O, Gritsenko PG, Bult P, Span PN, Friedl P. 2017. *Clin. Exp. Metastasis* 34(6–7):421–29
59. Padmanabhan V, Krol I, Suhail Y, Szczerba BM, Aceto N, et al. 2019. *Nature* 573(7774):439–44
60. van Neerven SM, Vermeulen L. 2023. *Nat. Rev. Mol. Cell Biol.* 24(3):221–36
61. Beedle AE, Roca-Cusachs P. 2023. *Curr. Opin. Cell Biol.* 84:102229
62. Balasubramaniam L, Monfared S, Ardaševa A, Rosse C, Schoenit A, et al. 2025. *Nat. Phys.* 21(2):269–78
63. Hohenberg PC, Halperin BI. 1977. *Rev. Mod. Phys.* 49(3):435–79
64. Zwicker D, Seyboldt R, Weber CA, Hyman AA, Jülicher F. 2016. *Nat. Phys.* 13(4):408–13
65. Bauermann J, Laha S, McCall PM, Jülicher F, Weber CA. 2022. *J. Am. Chem. Soc.* 144(42):19294–304
66. Abercrombie M, Heasman JE. 1954. *Exp. Cell Res.* 6(2):293–306
67. Abercrombie M, Ambrose E. 1958. *Exp. Cell Res.* 15(2):332–45
68. Carlier MF, Pantaloni D. 1997. *J. Mol. Biol.* 269(4):459–67
69. Pollard TD, Cooper JA. 2009. *Science* 326(5957):1208–12
70. Yam PT, Wilson CA, Ji L, Hebert B, Barnhart EL, et al. 2007. *J. Cell Biol.* 178(7):1207–21
71. O’Byrne J, Kafri Y, Tailleur J, van Wijland F. 2022. *Nat. Rev. Phys.* 4(3):167–83
72. Ramaswamy S. 2010. *Annu. Rev. Condens. Matter Phys.* 1:323–45
73. Bechinger C, Di Leonardo R, Löwen H, Reichhardt C, Volpe G, Volpe G. 2016. *Rev. Mod. Phys.* 88(4):045006
74. Doostmohammadi A, Thampi SP, Saw TB, Lim CT, Ladoux B, Yeomans JM. 2015. *Soft Matter* 11(37):7328–36
75. Hallatschek O, Datta SS, Drescher K, Dunkel J, Elgeti J, et al. 2023. *Nat. Rev. Phys.* 5(7):407–19
76. Solon AP, Cates ME, Tailleur J. 2015. *Eur. Phys. J. Spec. Top.* 224(7):1231–62
77. Martin D, O’Byrne J, Cates ME, Fodor E, Nardini C, et al. 2021. *Phys. Rev. E* 103(3):032607
78. Fodor t, Jack RL, Cates ME. 2022. *Annu. Rev. Condens. Matter Phys.* 13(1):215–38
79. Peyret G, Mueller R, d’Alessandro J, Begnaud S, Marcq P, et al. 2019. *Biophys. J.* 117(3):464–78
80. Amiri A, Mueller R, Doostmohammadi A. 2022. *J. Phys. A Math. Theor.* 55(9):094002
81. Tan TH, Mietke A, Li J, Chen Y, Higinbotham H, et al. 2022. *Nature* 607(7918):287–93
82. Irving JH, Kirkwood JG. 1950. *J. Chem. Phys.* 18(6):817–29
83. Christoffersen J, Mehrabadi MM, Nemat-Nasser S. 1981. *J. Appl. Mech.* 48(2):339–44
84. Korteweg D. 1901. *Arch. Néerl. Sci. Exactes Nat.* 6:1–24
85. Anderson D, McFadden G. 1997. *Diffuse-interface methods in fluid mechanics*. Tech. Rep. NISTIR 6018, US Department of Commerce
86. Monfared S, Zhou T, Andrade JE, Ioannidou K, Radjaï F, et al. 2020. *Phys. Rev. Lett.* 125(25):255501
87. Chiang M, Hopkins A, Loewe B, Marenduzzo D, Marchetti MC. 2024. *Phys. Rev. E* 110(4):044403
88. Puggioni L, Krommydas D, Giomi L. 2025. Preprint, arXiv:2502.09554v1 [cond-mat.soft]
89. Happel L, Voigt A. 2024. *Phys. Rev. Lett.* 132(7):078401
90. Monfared S, Ravichandran G, Andrade JE, Doostmohammadi A. 2024. *J. R. Soc. Interface* 21(214):20240022
91. Graham JN, Zhang G, Yeomans JM. 2024. *Soft Matter* 20(13):2955–60
92. Doostmohammadi A, Ladoux B. 2022. *Trends Cell Biol.* 32(2):140–50
93. Bowick MJ, Fakhri N, Marchetti MC, Ramaswamy S. 2022. *Phys. Rev. X* 12(1):010501
94. Shankar S, Souslov A, Bowick MJ, Marchetti MC, Vitelli V. 2022. *Nat. Rev. Phys.* 4(6):380–98
95. Barberis L, Condat CA, Faisal SM, Lowenstein PR. 2024. *Sci. Rep.* 14(1):25435
96. de Gennes PG, Prost J. 1993. *The Physics of Liquid Crystals*. Clarendon Press
97. Nelson D, Piran T, Weinberg S. 2004. *Statistical Mechanics of Membranes and Surfaces*. World Scientific. 2nd ed.
98. Ardaševa A, Doostmohammadi A. 2022. *Nat. Rev. Phys.* 4(6):354–56
99. Saw TB, Doostmohammadi A, Nier V, Kocgozlu L, Thampi S, et al. 2017. *Nature* 544(7649):212–16
100. Balasubramaniam L, Doostmohammadi A, Saw TB, Narayana GHNS, Mueller R, et al. 2021. *Nat. Mater.* 20(8):1156–66
101. Pérez-González C, Alert R, Blanch-Mercader C, Gómez-González M, Kolodziej T, et al. 2018. *Nat. Phys.* 15(1):79–88



102. Kawaguchi K, Kageyama R, Sano M. 2017. *Nature* 545(7654):327–31
103. Armengol-Collado JM, Carenza LN, Giomi L. 2024. *eLife* 13:e86400
104. Zhang G, Mueller R, Doostmohammadi A, Yeomans JM. 2020. *J. R. Soc. Interface* 17(169):20200312
105. Maroudas-Sacks Y, Garion L, Shani-Zerbib L, Livshits A, Braun E, Keren K. 2021. *Nat. Phys.* 17(2):251–59
106. Krommydas D, Carenza LN, Giomi L. 2023. Preprint, arXiv:2307.12956v3 [cond-mat.soft]
107. Nelson DR, Halperin BI. 1979. *Phys. Rev. B* 19(5):2457–84
108. Chiang M, Hopkins A, Loewe B, Marchetti MC, Marenduzzo D. 2024. *PNAS* 121(40):e2319310121
109. Vafa F, Nelson DR, Doostmohammadi A. 2024. *Phys. Rev. E* 109(6):064606
110. Happel L, Voigt A. 2024. *Phys. Rev. Lett.* 132(7):078401
111. Weinstein JA, Regev A, Zhang F. 2019. *Cell* 178(1):229–41.e16
112. Gupta VK, Chaudhuri O. 2022. *Trends Cell Biol.* 32(9):773–85
113. Schreck CF, Fusco D, Karita Y, Martis S, Kayser J, et al. 2023. *PNAS* 120(11):e2208361120
114. Zhang X, Zhang S, Wang T. 2022. *Stem Cell Res. Ther.* 13(1):415
115. Jason Gao GJ, Holcomb MC, Thomas JH, Blawzdziewicz J. 2016. *J. Phys. Condens. Matter* 28(41):414021
116. Sharma R, Karmakar S. 2025. *Nat. Phys.* 21(2):253–61
117. Zheng JY, Han SP, Chiu YJ, Yip AK, Boichat N, et al. 2017. *Biophys. J.* 113(7):1585–98
118. Sonin AA. 2004. *PNAS* 101(23):8525–26
119. Marquez-Florez K, Arroyave-Tobón S, Linares JM. 2023. *Mater. Des.* 225:111466
120. Chugh P, Clark AG, Smith MB, Cassani DA, Dierkes K, et al. 2017. *Nat. Cell Biol.* 19(6):689–97
121. Taneja N, Bersi MR, Baillargeon SM, Fenix AM, Cooper JA, et al. 2020. *Cell Rep.* 31(1):107477
122. Arciero JC, Mi Q, Branca MF, Hackam DJ, Swigon D. 2011. *Biophys. J.* 100(3):535–43
123. Cochet-Escartin O, Ranft J, Silberzan P, Marcq P. 2014. *Biophys. J.* 106(1):65–73
124. Priest AV, Sivasankar S. 2023. Characterizing the Biophysical Properties of Adhesive Proteins in Live Cells Using Single-Molecule Atomic Force Microscopy. In *Mechanobiology: Methods and Protocols*. Springer
125. Trichet L, Le Digabel J, Hawkins RJ, Vedula SRK, Gupta M, et al. 2012. *PNAS* 109(18):6933–38
126. Tan SJ, Chang AC, Anderson SM, Miller CM, Prahl LS, et al. 2020. *Sci. Adv.* 6(20):eaax0317
127. Peyret G, Mueller R, d’Alessandro J, Begnaud S, Marcq P, et al. 2019. *Biophys. J.* 117(3):464–78
128. Du Roure O, Saez A, Buguin A, Austin RH, Chavrier P, et al. 2005. *PNAS* 102(7):2390–95
129. Blanch-Mercader C, Yashunsky V, Garcia S, Duclos G, Giomi L, Silberzan P. 2018. *Phys. Rev. Lett.* 120(20):208101
130. Zhang G, Yeomans JM. 2023. *Phys. Rev. Lett.* 130(3):038202
131. Wang W, Law RA, Perez Ipiña E, Konstantopoulos K, Camley BA. 2025. *PRX Life* 3(1):013012
132. Ritter CM, Ma T, Leijnse N, Barooji YF, Brickman JM, et al. 2025. *Phys. Rev. Lett.* 134(16):168401
133. Schoenit A, Monfared S, Anger L, Rosse C, Venkatesh V, et al. 2025. *Nat. Mater.* 24(6):966–76
134. Lauffenburger DA, Horwitz AF. 1996. *Cell* 84(3):359–69
135. d’Alessandro J, Barbier-Chebbah A, Cellerin V, Benichou O, Mège RM, et al. 2021. *Nat. Commun.* 12(1):4118
136. Perez Ipiña E, d’Alessandro J, Ladoux B, Camley BA. 2024. *PNAS* 121(22):e2318248121
137. Maître JL, Berthoumieu H, Krems SFG, Salbreux G, Jülicher F, et al. 2012. *Science* 338(6104):253–56
138. Manning ML, Fots RA, Steinberg MS, Schoetz EM. 2010. *PNAS* 107(28):12517–22
139. Niessen CM, Gumbiner BM. 2002. *J. Cell Biol.* 156(2):389–400
140. Heisenberg CP, Bellaïche Y. 2013. *Cell* 153(5):948–62
141. Kuang X, Guan G, Wong MK, Chan LY, Zhao Z, et al. 2022. *PLOS Comput. Biol.* 18(1):e1009755
142. Mo CK, Liu J, Chen S, Storrs E, Targino da Costa ALN, et al. 2024. *Nature* 634(8036):1178–86
143. Romani P, Valcarcel-Jimenez L, Frezza C, Dupont S. 2021. *Nat. Rev. Mol. Cell Biol.* 22(1):22–38
144. Camley BA, Zhang Y, Zhao Y, Li B, Ben-Jacob E, et al. 2014. *PNAS* 111(41):14770–75
145. Moure A, Gomez H. 2020. *Biomech. Model. Mechanobiol.* 19(5):1491–508
146. Chojowski R, Schwarz US, Ziebert F. 2024. *Soft Matter* 20(22):4488–503
147. Najem S, Grant M. 2016. *Phys. Rev. E* 93(5):052405
148. Li Y, Konstantopoulos K, Zhao R, Mori Y, Sun SX. 2020. *J. Cell Sci.* 133(20):jcs240341

149. Shelley MJ. 2024. *Phys. Rev. Fluids* 9(12):120501
150. Sun H. 2024. *Three-dimensional modeling of active cell assemblies*. PhD Thesis, University of Copenhagen
151. Link R, Jaggy M, Bastmeyer M, Schwarz US. 2024. *PLOS Comput. Biol.* 20(4):e1011412
152. Zehnder SM, Suaris M, Bellaire MM, Angelini TE. 2015. *Biophys. J.* 108(2):247–50
153. Jipp M, Wagner BD, Egbringhoff L, Teichmann A, Rübeling A, et al. 2024. *Cell Rep.* 43(8):114553
154. Tanida S, Fuji K, Lu L, Guyomar T, Lee BH, et al. 2024. Preprint, *bioRxiv*:2024.04.22.590518

